Journal of Civil Engineering and Construction 2025;14(4):188-199
https://doi.org/10.65720/jcec.2025.14.4.188

Characterization of spatial and temporal evolution of saltwater intrusion in the Qingnian reservoir of Pinglu Canal

Jianghua Liao[1], Keqin Xu[1], Shengfa Yang[2]*, Jiang Hu[2], Bo Xie[1], Geng Li[2], Peng Wu[3], Huaihan Liu[4]

1.School of River and Ocean Engineering, Chongqing Jiaotong University, Chongqing 400074, China;
2.National Engineering Research Center for Inland Waterway Regulation, Chongqing Jiaotong University, Chongqing 400074, China
3. CCCC Water Transportation Consultants Co., Ltd., Beijing 100007, China;
4.Changiang Waterway Bureau,Wuhan 430010;
E-mail: ysf777@163.com (S. Yang).

Received: 2 November 2025; Accepted: 22 December 2025; Available online: 31 December 2025

Abstract: After the construction of the Pinglu Canal, the operation of the ship lock induces saltwater intrusion into the Qingnian Reservoir, threatening the drinking water supply of Qinzhou City. Despite its significance, studies on the dynamics of low-salinity and non-tidal saltwater intrusion in large artificial canal-reservoir systems remain limited. This study therefore establishes a three-dimensional hydrodynamic and salinity transport numerical model validated against field measurements and laboratory experiments, with discrepancies of less than 0.05 m for water levels and 4% for salinity transport, to systematically investigate the spatiotemporal evolution of saltwater intrusion in the Qingnian Reservoir.This work provides novel insights by quantifying the relationship between upstream inflow and intrusion distance, and by deriving specific operational criteria for drinking-water safety based on stratification analysis.The results show that saltwater intrusion displays a distinct salt-wedge pattern, with the bottom saline layer intruding up to 7.54 km. The maximum intrusion distance is positively correlated with the salinity boundary at the upstream approach channel and negatively correlated with upstream inflow. Specifically, a 411% increase in runoff (from 21.8 to 111.3 m^3/s) reduces the intrusion distance by 70% (5.36 km), indicating that higher upstream discharge effectively suppresses the upstream advance of saltwater.Density-driven vertical salinity stratification develops, with the stratification coefficient increasing along the intrusion path. Specifically, safety-margin analysis confirms that under upstream salinity-boundary conditions of 1‰ to 3‰, the use of surface water intakes can reliably maintain output salinity within permissible limits. The research results provide a theoretical basis and technical support for the water resource safety of large-scale estuarine canal projects.
Keywords: Pinglu Canal; Saltwater intrusion; Salinity stratification; Numerical simulation.

1.Introduction

Lock complexes connecting marine and inland water systems, while delivering enormous navigational benefits, have induced saltwater intrusion as a prevalent environmental issue threatening the water quality safety of reservoir areas, protection of drinking water sources, and agricultural irrigation[[1-[5]. This problem widely exists globally. For example, multiple locks in the Netherlands' Delta Works have long been coping with saltwater intrusion from the North Sea [6-8]; the lock systems along the U.S. Gulf Coast have also led to the degradation of upstream freshwater ecosystems due to saltwater intrusion [9-11]; numerous lock complexes at the Yangtze River Estuary and Pearl River Estuary in China are similarly facing varying degrees of salt tide upstream intrusion risks [12-16]. Saltwater intrusion continuously propagates upstream through locks as an "artificial channel", posing a direct threat to freshwater resource ecosystems. Therefore, in - depth research on the spatiotemporal evolution patterns of saltwater intrusion in reservoirs holds significant theoretical value and urgent engineering demand.

As a national strategic project connecting the Xijiang River Basin and Qinzhou Port in Beibu Gulf, the Pinglu Canal has drawn great attention to the water safety of its Qingquan Reservoir section [3,17]. Compared with typical estuarine locks, the Qingquan lock of the Pinglu Canal has its own uniqueness: first, the lock is far from the estuary, and the salinity of seawater has been significantly reduced when it intrudes into the downstream approach channel after long - distance river dilution; second, as a large - scale regulating reservoir, the water environment of

Qingquan Reservoir is weakly affected by tidal dynamics, and the saltwater intrusion process is mainly controlled by the dynamic confrontation between lock discharge and upstream runoff [18,[19]. After the completion of the Pinglu Canal, Qingquan Reservoir will become an important drinking water source and agricultural irrigation source for Qinzhou City in the future, and its water quality safety is directly related to the regional social and economic development and ecological stability. Although salt - prevention measures have been considered in the engineering design, making the salinity boundary at the exit of the upstream approach channel controlled within a relatively low range (1-3‰), far lower than the intrusion salinity of 15-35‰ in foreign sea locks[20], with the long - term and frequent operation of the lock, saltwater will still continuously propagate upstream into the reservoir area, forming a stable low - salinity saltwater wedge. Therefore, for the lock - reservoir system under the background of river - sea combined transport, with low salinity and without tidal influence, conducting research on its saltwater upstream intrusion patterns and distribution characteristics is of great theoretical and practical significance for ensuring the health of the reservoir ecosystem, achieving refined water resource management, and safe utilization.

Currently, domestic and international scholars have conducted extensive research on such estuarine saltwater intrusion problems. In terms of theoretical models and physical experiments, early studies, represented by the classic works of Keulegan GH et al.[21] and Benjamin TB[22], established empirical relationships between the head velocity of density currents and the Richardson number through flume experiments and theoretical derivations, and constructed a theoretical framework for motion under ideal conditions. Building on this, scholars such as Simpson JE [23] and Turner JS [24] deeply revealed the vortex structures and entrainment mechanisms of the density current head through detailed experiments. Domestic scholars like Li YZ [25] and Zhou HX [26] were among the first to conduct in - situ observations and calculate intrusion volumes. In recent years, research has further deepened into complex boundary conditions. For example, Yin X et al [27] and Lin YD et al. [28][30] explored the effects of long - lock exchange, vegetation groups, and bed roughness on the evolution laws of density currents, respectively. It is particularly worth mentioning that, targeting the unique hydrodynamic disturbances caused by lock operation, Xu KQ et al. [31],[32] systematically studied the effects of ship movement and propeller wake on the structural evolution of saltwater density currents and the salt - fresh water mixing process through high - precision PIV - Plif flume experiments. They revealed the influence mechanism of ship navigation in estuaries on saltwater intrusion, providing new perspectives for lock scheduling and salt - prevention design. In terms of numerical simulation technology, with the leap in computing power, research has developed from early two - dimensional models to high - resolution three - dimensional simulations [33]. Researchers adopt methods such as RANS, LES, LBM, and even DNS to precisely capture the flow field structures and mixing processes of density currents [33-[36]. For instance, Liang XL et al. [34] used DNS to analyze energy conversion in stratified environments, while Cantero MI et al. [35],[36] reproduced the complex vortex structures of the density current head. Xu KQ et al. [37] adopted the LBM method to reveal the influence laws of salinity difference and water depth on saltwater intrusion distance. At the engineering application level, Huang C etal. [38] and Ding L et al. [39] constructed salinity models for large estuaries such as the Yangtze River Estuary, evaluating the impact of engineering and hydrological factors on intrusion. Furthermore, numerical studies by scholars such as Dai A et al. [40],[41] and Zhu R et al. [42] in aspects such as gravity current mixing, energy budget, and collision processes have further promoted the development of this field towards multi - physical field coupling and high - precision prediction.

However, existing studies have predominantly focused on typical estuaries with significant tidal dynamic effects and relatively high salinity. In contrast, for the saltwater intrusion problem in inland ship locks like the Qingquan Reservoir of the Pinglu Canal, which is characterized by relatively low salinity, without direct tidal influence, and constrained by reservoir topography, systematic and in - depth research on its unique dynamic mechanisms and evolutionary characteristics is still lacking. Particularly, under low - salinity boundary conditions, there remain numerous scientific questions that urgently need to be addressed, such as how the salinity stratification structure responds, how the intrusion distance can be accurately predicted, and how to formulate scheduling strategies that balance navigation and water safety.

Given this, this paper takes the Qingquan Reservoir of the Pinglu Canal as the research object and adopts a validated 3D hydrodynamic - salinity transport mathematical model to systematically investigate the spatiotemporal evolutionary characteristics of saltwater intrusion in the reservoir area under different salinity boundary conditions. The main objects of this paper : Section 2 provides a detailed introduction to the model construction and validation process. Section 3 presents the results and analysis. Among them, Section 3.1 reveals the saltwater intrusion patterns in the Qingquan Reservoir area; Section 3.2 quantitatively analyzes the vertical stratification structure; Section 3.3 assesses the water intake safety in the reservoir area; Section 3.4 conducts an in - depth discussion on the simulation results, compares them with existing theories, and analyzes the innovation and limitations of this study. Section 4 summarizes the main conclusions of the whole paper and puts forward future research prospects.

2.Model Construction and Validation

2.1 Model Construction

Considering the complex riverine terrain of the Qingquan Reservoir, this study employs the MIKE 3 model. Its governing equations include the mass conservation, momentum, and salt transport equations, which are solved using the Boussinesq approximation and a baroclinic module. The standard k-ε turbulence closure model is adopted to calculate the vertical eddy viscosity and diffusivity coefficients. For detailed computational principles, refer to the works of Xu Keqin [17] and Xiao Yi [3].

Based on the proposed navigation channel engineering plan, a three-dimensional (3D) numerical model was developed to simulate saltwater intrusion in the Qingquan Reservoir post-construction. As shown in Figure 1, the model domain covers the Qingquan Hub sluice gates, the Qingquan Reservoir, the upstream navigation channel, and the old Qinjiang River course. The domain spans 16.7 km in the east-west direction and 17.1 km in the north-south direction, with a navigation channel length of approximately 27.1 km. An unstructured triangular mesh with a resolution of 30 m was utilized. Vertically, the model uses a sigma coordinate system, equally divided into 5 sigma layers, resulting in a total of 218,240 grid cells. The model is georeferenced to the China Geodetic Coordinate System 2000 (CGCS2000), with elevations based on the National Vertical Datum 1985.

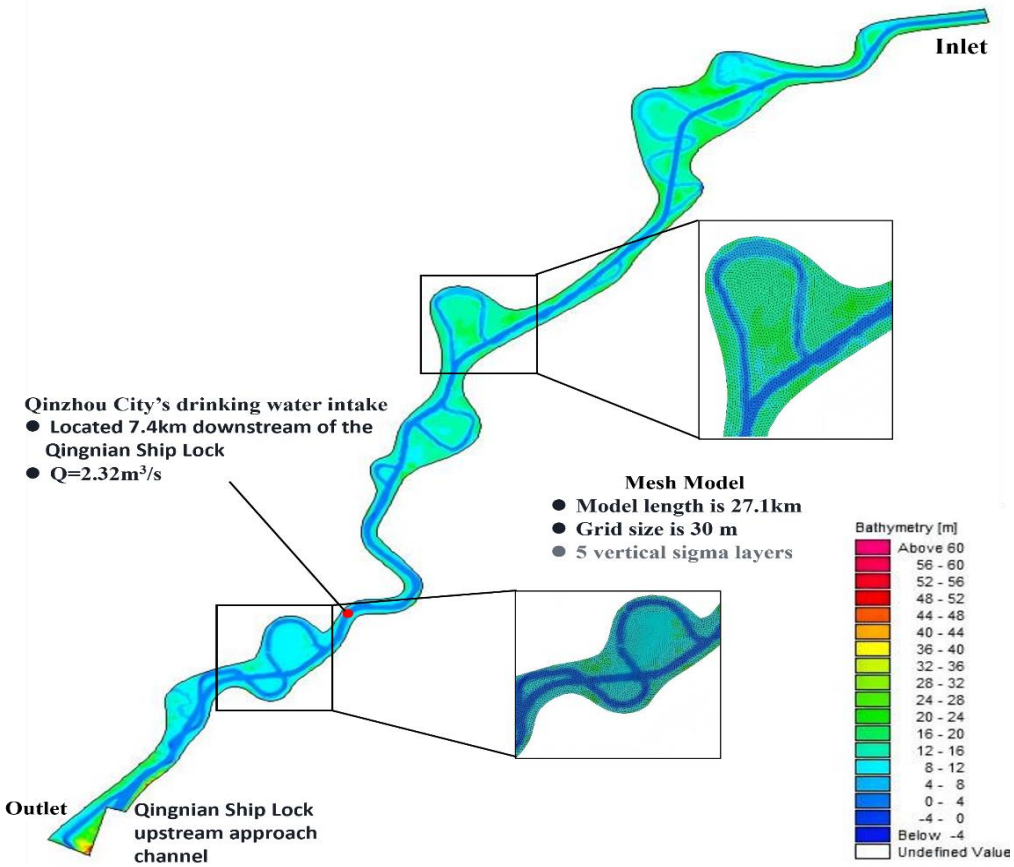

Figure 1. Schematic of the computational model setup. (The model domain has a total length of 27.12 km with a 30 m mesh resolution and 5 vertical sigma layers. The Dafengjiang water intake is located 7.4 km upstream of the Qingquan Sluice Gate, with a withdrawal rate of 2.32 m³/s)

2.2 Computational Conditions and Scenarios

The extent of saltwater intrusion in the Qingquan Reservoir is jointly influenced by freshwater discharge and the salinity at the exit of the approach channel. Unlike the high-salinity intrusion (15-35‰) typical of foreign sea locks, the saltwater intrusion at the Qingquan Lock is characterized by lower salinity levels.

In this study, the upstream flow boundary of the model was defined by the dry-season discharge from the Pinglu Canal project, corresponding to a 90% guarantee rate in the near term (Figure 2). The downstream hydrodynamic boundary was specified using the normal pool level of 8.7 m at the Qingquan Hub. A salinity boundary was applied at the exit of the upstream approach channel of the Qingquan Lock. Based on the findings of Xiao Yi et al. [3][17],

which indicate that the salinity at this location remains below 3‰ when anti-salinity measures are implemented, this study investigates four specific boundary conditions: 1‰, 1.5‰, 2‰, and 3‰. The objective is to analyze the patterns of saltwater intrusion in the Qingquan Reservoir under these varying salinity conditions.

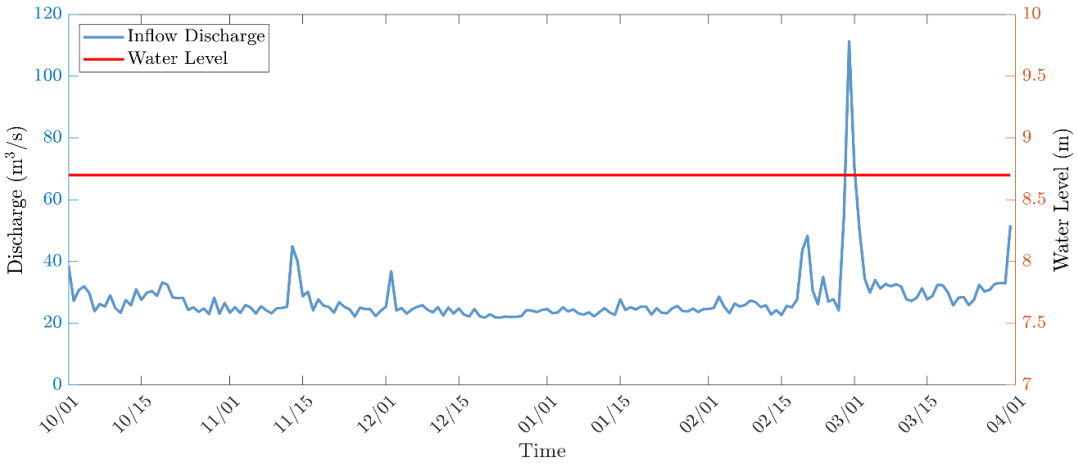

Figure 2. Upstream flow and downstream water level for the 90% guarantee rate.

A total of four scenarios were established, with salinity boundaries at the upstream approach channel set to 1‰, 1.5‰, 2‰, and 3‰, respectively (Table 1). The simulation period covered the entire dry season (from October 1 to March 31 of the following year), for a total duration of 182 days.

Table 1. Summary of simulation scenarios

Case	Flow Guarantee Rate	Simulation Period (Duration)	Salinity at Upstream Approach Channel Exit (‰)
Case1	90%	Oct 1 – Mar 31 (182 days)	1‰
Case2			1.5‰
Case3			2‰
Case4			3‰

2.3 Model Validation

(1) Hydrodynamic Validation

The hydrodynamic model was validated against the measured water surface profile under multi-year average flow conditions, with an inlet flow of 62.8 m³/s and an outlet water level of 8.7 m. The discrepancy between the simulated and measured water levels was within 0.05 m, demonstrating the model's capability to accurately reproduce the hydrodynamic characteristics of the reservoir (Figure 3).

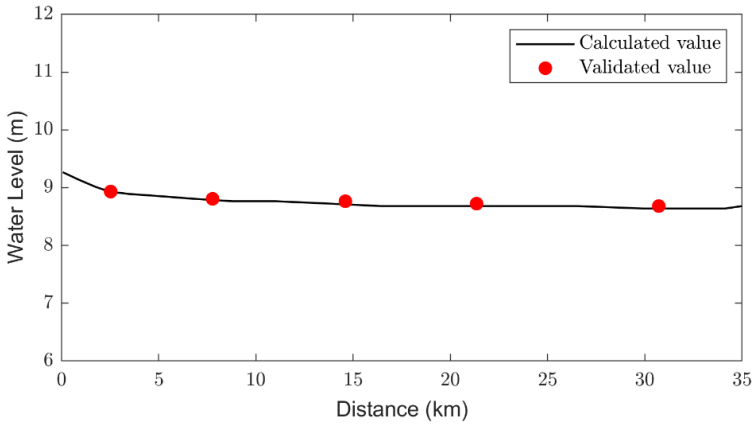

Figure 3. Validation of water levels

(2) Salinity Transport Validation

As pre-project saltwater could not intrude into the Qingquan Reservoir, on-site measured data were unavailable. Therefore, this study validates the model's salinity transport module using data from a flume experiment cited in reference[43]. The rectangular experimental flume measured 110 m in length, 0.5 m in width, and 0.5 m in height. The experiment investigated saltwater movement under conditions with runoff but no tide, which are similar to the saltwater intrusion conditions in the Qingquan Reservoir after the Pinglu Canal project. For details on the validation cases and results, see Xu [17] (2025). The model was validated against five salinity transport cases with different salinities and flow rates. The maximum saltwater intrusion distance from the numerical simulation was close to the experimental results, with an error of less than 4%. Furthermore, the trend of saltwater intrusion distance over time was consistent with the experimental data, showing an error of less than 10%. These results confirm the reliability of the model (Table 2).

Table 2. Comparison of experimental parameters and maximum saltwater intrusion distances

Case	Water Depth （m）	Freshwater Flow Rate （m³/s）	Salinity （‰）	Max. Intrusion Distance (Flume) (m)	Max. Intrusion Distance (Model) (m)	Difference in Maximum Intrusion Distance (m)	Relative Error （m）
1	0.25	15	17.7	75.5	76.3	-0.8	-1.06%
2	0.25	15	10.2	52	52.8	-0.8	-1.54%
3	0.25	12.4	10.2	73	72.6	0.4	0.55%
4	0.2	9	10	68	67.8	0.2	0.29%
5	0.22	15	10.9	28	28.9	-0.9	-3.21%

3.Results

3.1 Characteristics of Saltwater Intrusion in the Qingquan Reservoir

Saltwater intrusion in the Qingquan Reservoir exhibits a typical saltwater wedge morphology. The longitudinal salinity distribution decreases progressively in the upstream direction, while the vertical profile is stratified, following the pattern of bottom > middle > surface layers. The intrusion length of the saltwater wedge is a key indicator for assessing the extent of saltwater intrusion, and its evolution is jointly controlled by the salinity boundary and upstream runoff.

Figure 4 shows the time series of the bottom-layer saltwater intrusion distance and runoff under various salinity boundary conditions. It is evident that the maximum saltwater intrusion distance is negatively correlated with the upstream runoff. As the runoff increases, the saltwater intrusion distance exhibits a significant decreasing trend, regardless of variations in the salinity boundary. This macroscopic phenomenon suggests that upstream runoff is the key factor inhibiting saltwater intrusion.

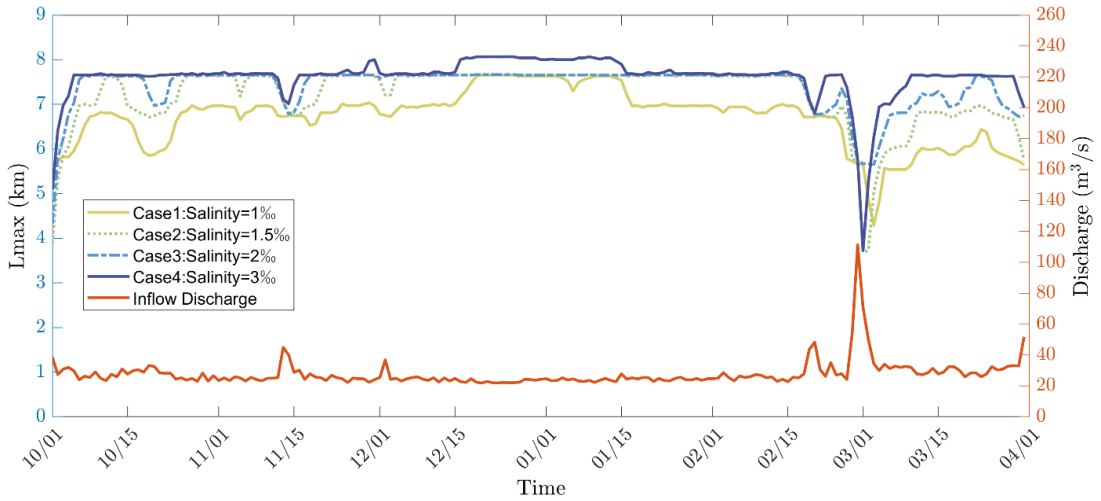

Figure 4. Time series of bottom-layer saltwater intrusion distance and upstream runoff under various salinity

boundary conditions (representing the 90% guarantee rate discharge process during the dry season).

To precisely quantify the impacts of runoff and the salinity boundary, this study compared the saltwater intrusion distances under two scenarios: minimum upstream flow (Q=21.8 m³/s, on December 20) and maximum upstream flow (Q=111.3 m³/s, on February 28). As shown in Figure 5, under the minimum flow condition, as the upstream salinity boundary increased from 1‰ to 3‰, the bottom-layer intrusion length monotonically increased from 7.5 km to 7.97 km, an increase of only 6.27%. This indicates that while the upstream salinity boundary is the source of buoyancy driving the intrusion, its magnitude of impact is relatively moderate. As shown in Figure 6, under the maximum flow condition, the saltwater intrusion distance was reduced to less than 3 km. Even with the high salinity boundary of 3‰, the intrusion distance was sharply reduced to 2.61 km—a reduction of 5.36 km compared to the minimum flow scenario, resulting in a saltwater intrusion suppression rate as high as 67.3%.

Quantitative comparison reveals that a 200% increase in the upstream salinity boundary (from 1‰ to 3‰) led to only a 6.27% increase in intrusion distance (an additional 0.47 km). In contrast, a 411% increase in runoff (from 21.8 to 111.3 m³/s) resulted in a 70% reduction in intrusion distance (a decrease of 5.36 km). Combined with the macroscopic pattern observed in Figure 4, this result clearly reveals that upstream runoff is the dominant factor controlling the length of saltwater intrusion in the Qingquan Reservoir, and its regulatory effect is orders of magnitude greater than that of the salinity boundary. Therefore, implementing a “freshwater flushing” strategy through the joint operation of upstream reservoirs is an effective engineering measure to ensure the security of the reservoir’s water resources.

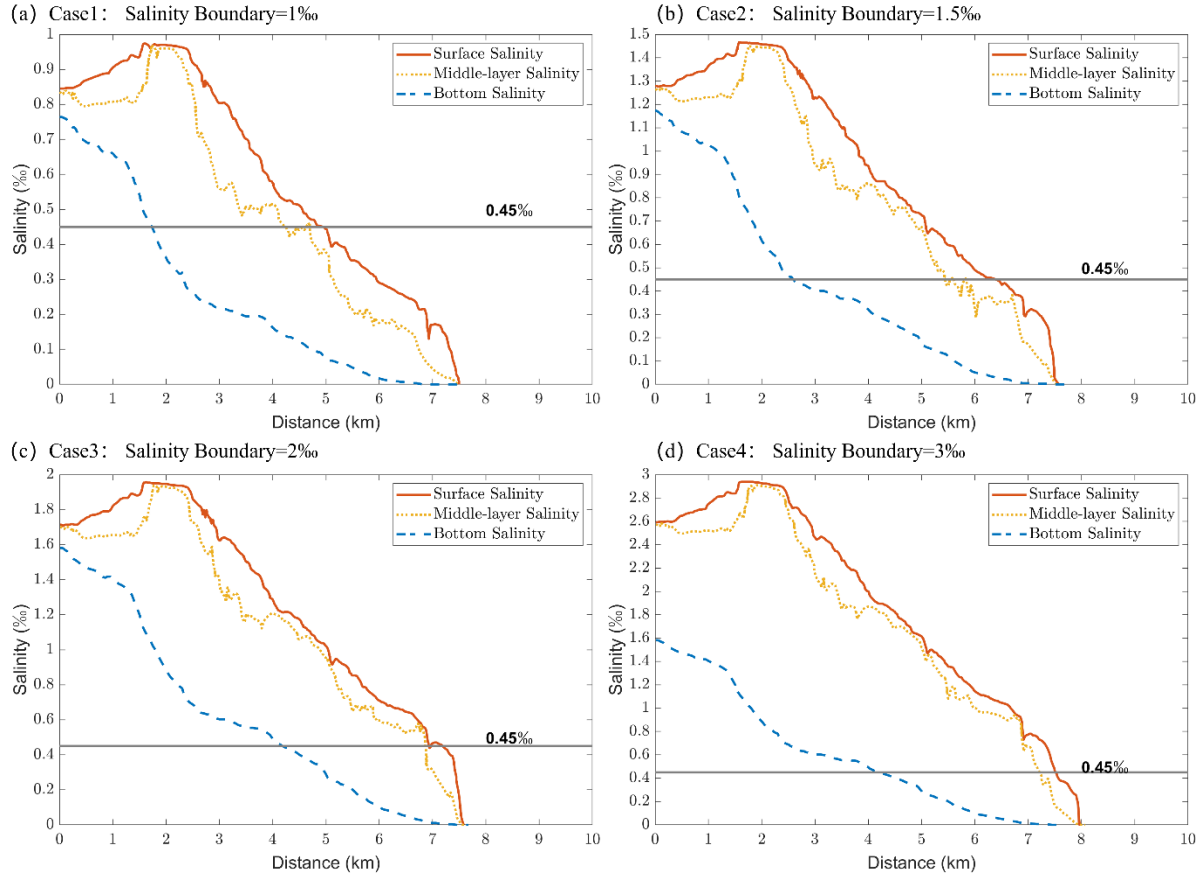

Figure 5. Longitudinal salinity distribution along the reservoir’s navigation channel centerline under minimum runoff conditions. (Upstream flow Q=21.8 m³/s, December 20;(a) 1‰ salinity boundary, maximum intrusion distance: 7.5 km;(b) 1.5‰ salinity boundary, maximum intrusion distance: 7.52 km;(c)2‰ salinity boundary, maximum intrusion distance: 7.58 km;(d)3‰ salinity boundary, maximum intrusion distance: 7.97 km)

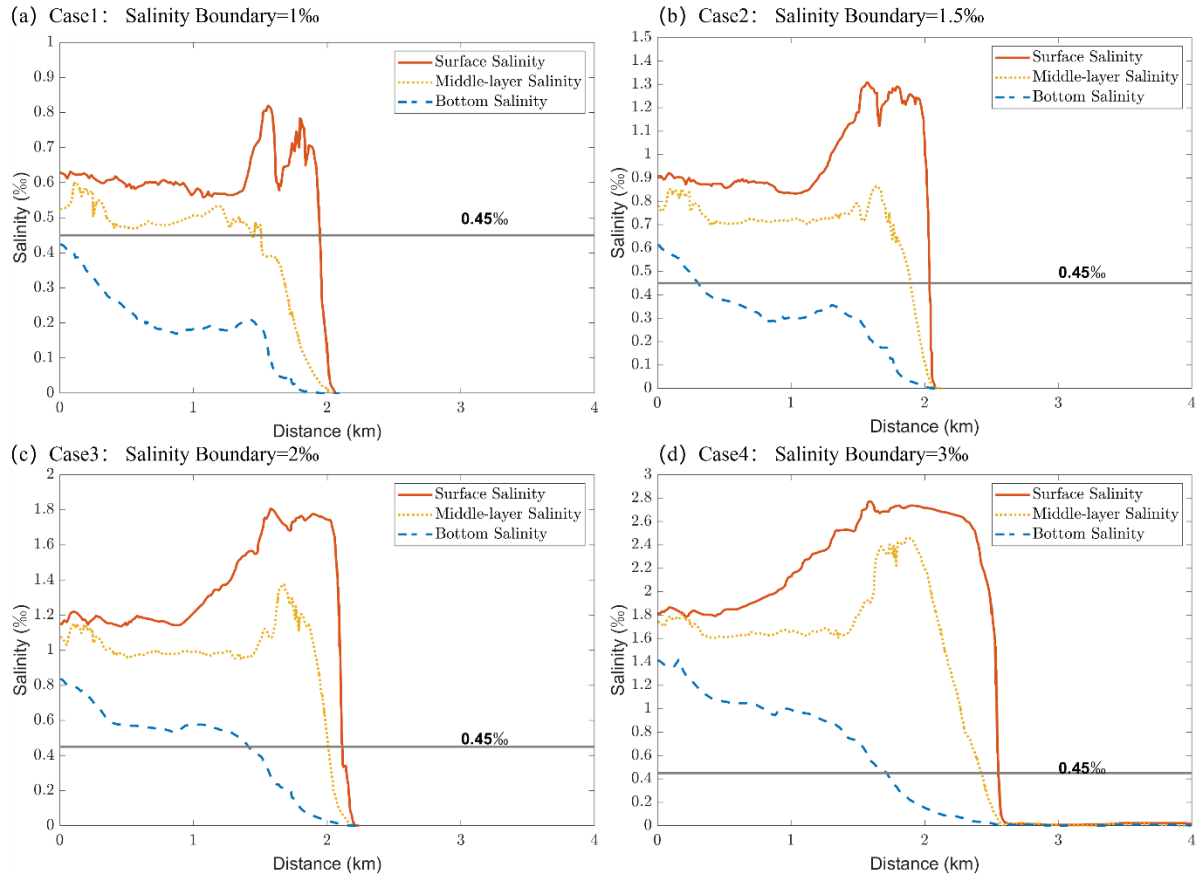

Figure 6. Longitudinal salinity distribution along the reservoir's navigation channel centerline under maximum runoff conditions. (Upstream flow Q=111.3 m³/s, February 28;(a) 1‰ salinity boundary, maximum intrusion distance: 2.04 km;(b) 1.5‰ salinity boundary, maximum intrusion distance: 2.08 km;(c) 2‰ salinity boundary, maximum intrusion distance: 2.15 km;(d) 3‰ salinity boundary, maximum intrusion distance: 2.61 km)

3.2 Vertical Stratification of Salinity and Its Quantification

The presence of the saltwater wedge leads to significant vertical stratification in the reservoir water body. To quantitatively assess the stratification intensity, the vertical salinity stratification coefficient is introduced, calculated as follows:

$$n = \frac{C_{bot} - C_{surf}}{C_{mean}} \tag{1}$$

Where C_{bot} represents the bottom - layer saltwater salinity, C_{surf} represents the surface - layer freshwater salinity, C_{mean} is the mean salinity, and n is the vertical salinity stratification coefficient.

Figure 7 illustrates the longitudinal variation of the stratification coefficient under low-flow conditions for different salinity boundaries. The analysis reveals that as the distance from the lock increases, the stratification coefficient (n) exhibits an increasing trend, indicating that the salinity stratification becomes more stable further upstream. The stratification coefficient (n) is negatively correlated with the salinity boundary. Under a low-salinity boundary (e.g., 1‰), the n value is relatively high despite a small absolute salinity difference, owing to the low mean salinity. Conversely, as the salinity boundary increases, the n value shows a decreasing trend. This reveals an important pattern: in a high-salinity environment, the rise in the overall salinity level of the water body weakens the relative stratification intensity. This finding is of great significance for understanding the mixing mechanisms in low-salinity environments.

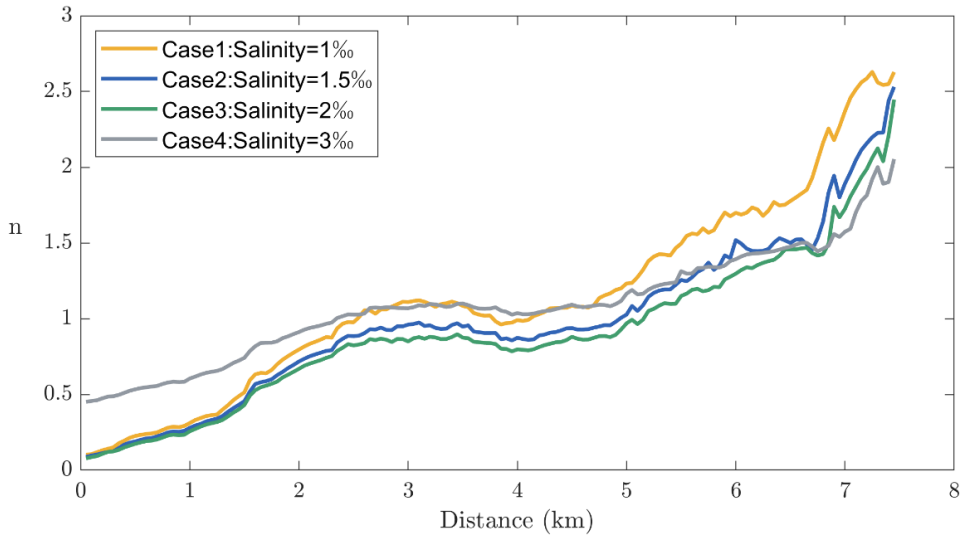

Figure 7. Longitudinal distribution of salinity stratification coefficient in the reservoir area under minimum runoff conditions (upstream flow rate Q=21.8 m³/s, December 20)

3.3 Assessment of Drinking Water Intake Safety for Qinzhou City

After the construction of the Pinglu Canal, the Qingquan Reservoir has become the drinking water source for Qinzhou City, making its water quality security of paramount importance. This study focuses on the Dafengjiang Intake, located 7.5 km downstream of the sluice gate (see Figure 1 for its specific location), with a time-averaged water intake rate of 2.32 m³/s. The paper employs the Margin of Safety (M) for quantitative assessment, defined as follows:

$$M = C_{std} - C_{\max} \tag{2}$$

Where C_{std} is the standard limit, which is 0.45‰ for drinking water according to national regulations, and $C_{\max}$ is the maximum calculated salinity at the intake.

Figure 8 presents the temporal evolution of vertical salinity at the Dafengjiang Intake under different salinity boundary conditions. It is evident that significant vertical stratification exists in the water body at the intake, and this stratification becomes more pronounced with higher salinity boundaries. Table 3 summarizes the maximum salinities in the bottom, middle, and surface layers, the cross-sectional average salinity, and the Margin of Safety for each scenario. A comprehensive review of the figures and table reveals that the Margin of Safety (M) varies significantly across different water layers and salinity boundaries. When the salinity boundary is controlled at or below 2‰, the Margin of Safety is positive for all water layers, indicating that the water intake is fully secure. Even under the extreme scenario of a 3‰ salinity boundary, the margins of safety for the surface and middle layers remain high at 0.43‰ and 0.11‰, respectively, fully complying with the standard. However, the Margin of Safety for the bottom layer is negative (-0.13‰), posing a risk of instantaneous exceedance.

This quantitative assessment clearly demonstrates that by leveraging the natural stratification of the water body and adopting a surface water intake strategy, it is possible to ensure that the salinity of the abstracted water remains far below the standard limit, even under the most unfavorable salinity boundary conditions. This provides an ample Margin of Safety and offers a reliable technical guarantee for the drinking water security of Qinzhou City.

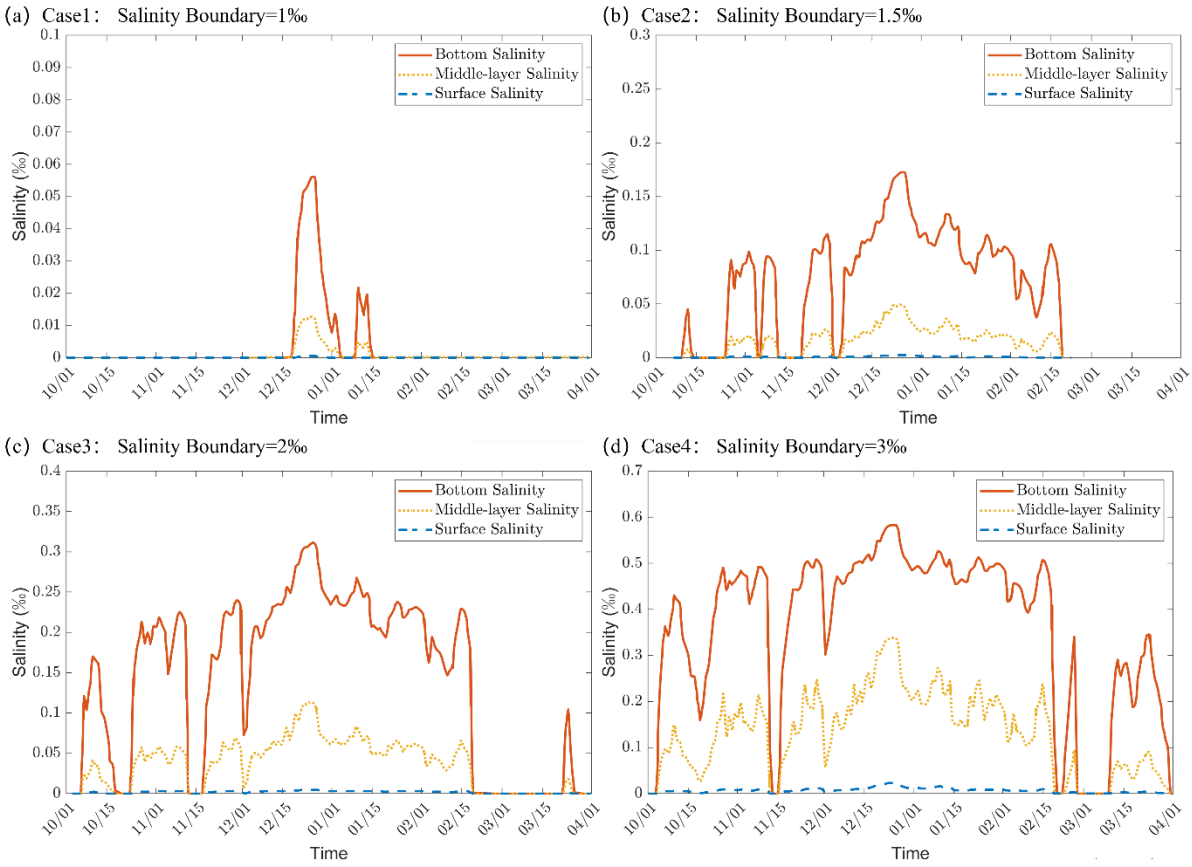

Figure 8. Water salinity distribution at the Qinzhou drinking water intake ((a) 1‰ salinity boundary, cross - sectional average salinity 0.023‰; (b) 1.5‰ salinity boundary, cross - sectional average salinity 0.075‰; (c) 2‰ salinity boundary, cross - sectional average salinity 0.144‰; (d) 3‰ salinity boundary, cross - sectional average salinity 0.316‰)

Table 3. Maximum salinity and margin of safety at the Qinzhou drinking water intake

Case	Salinity Boundary (‰)	Water Layer	Max. Salinity (‰)	Margin of Safety (M)	Date of Occurrence
1	1	Surfae	0.001	0.449	Dec 25
		Middle	0.013	0.437	Dec 25
		Bottom	0.056	0.394	Dec 26
		Cross-sectional Avg.	0.023	0.427	Dec 25
2	1.5	Surfae	0.003	0.447	Dec 26
		Middle	0.050	0.4	Dec 24
		Bottom	0.173	0.277	Dec 25
		Cross-sectional Avg.	0.075	0.375	Dec 25
3	2	Surfae	0.005	0.445	Dec 25
		Middle	0.114	0.336	Dec 24
		Bottom	0.312	0.138	Dec 25
		Cross-sectional Avg.	0.144	0.306	Dec 25
4	3	Surfae	0.024	0.426	Dec 25
		Middle	0.339	0.111	Dec 25
		Bottom	0.584	-0.134	Dec 25
		Cross-sectional Avg.	0.316	0.134	Dec 25

3.4 Disscussion

Through 3D numerical simulation, this study systematically reveals the patterns of saltwater intrusion in the Qingquan Reservoir following the Pinglu Canal project and its impact on water intake safety. The conclusions drawn are highly consistent with classical saltwater wedge theory, while also exhibiting unique characteristics influenced by the specific project conditions.

Firstly, the study confirms that upstream runoff is the dominant factor in inhibiting saltwater intrusion, with its regulatory effect being orders of magnitude greater than that of the salinity boundary at the lock outlet. This finding aligns with the theoretical relationship proposed by Keulegan et al., which states that the saltwater wedge length is inversely proportional to the square of the densimetric Froude number [21]. In this study, the increase in runoff directly enhances the flow's inertial force, effectively suppressing the buoyancy-driven effect caused by the density difference, thereby significantly shortening the intrusion distance. This quantitative comparison provides direct theoretical support for reservoir operation and management: during dry periods, implementing a "freshwater flushing" strategy through the joint operation of upstream reservoirs is an effective strategy for ensuring the water resource security of the Qingquan Reservoir.

Secondly, the vertical salinity stratification coefficient introduced in this study quantifies the stratification structure of the water body, revealing the phenomenon that the relative stratification intensity weakens as the salinity boundary increases. This deepens the understanding of mixing mechanisms in low-salinity environments and provides a physical basis for the scientific validity of the surface water intake strategy.

Furthermore, this study combines the macro-scale patterns of saltwater intrusion with the micro-scale response at the water intake to conduct a Margin of Safety assessment, achieving a progression from phenomenological description to risk assessment. The results indicate that, due to its considerable distance and the benefit of significant stratification effects, the Qinzhou drinking water intake can still maintain an ample Margin of Safety through surface water extraction, even under the extreme 3‰ salinity boundary condition.

Of course, this study has certain limitations, as it did not consider the effects of factors such as the transient processes of single lock operations, short-term flow fluctuations, or ship navigation. Future research could involve more refined and detailed simulation studies.

4.Conclusion

By developing a 3D hydrodynamic-salinity numerical model for the Qingquan Reservoir of the Pinglu Canal, this study systematically reveals the spatiotemporal evolution patterns of saltwater intrusion and its impact on intake safety. The main conclusions are as follows:

1) The saltwater intrusion in the Qingquan Reservoir exhibits a typical saltwater wedge morphology. The bottom-layer saltwater intrusion distance is positively correlated with the salinity boundary and negatively correlated with the upstream runoff. Upstream runoff is the dominant factor controlling the intrusion length, and its regulatory effect is far greater than the impact of the salinity boundary. Increasing the upstream discharge is an effective engineering measure to suppress saltwater intrusion.

2) Significant vertical salinity stratification exists in the reservoir water body, with the salinity distribution following the pattern of bottom > middle > surface layers. The relative stratification intensity weakens as the salinity boundary increases, while the stratification stability strengthens with increasing intrusion distance.

3) The Margin of Safety assessment for the Qinzhou drinking water intake indicates that under salinity boundary conditions ranging from 1‰ to 3‰, adopting a surface water intake strategy can ensure that the abstracted water salinity meets drinking water standards, providing a sufficient safety guarantee.

The findings of this study not only reveal the intrinsic mechanisms of saltwater intrusion in the Pinglu Canal's Qingquan Reservoir but also provide a direct theoretical basis and technical support for safeguarding the drinking water safety of Qinzhou City. They hold significant reference value for water resource management in similar large-scale estuarine canal projects.

5.Acknowledgments

This study was supported by the National Key Research and Development Program of China (No. 2023YFC3208803).

6. References

[1] Werner AD, Simmons CT. Impact of sea-level rise on sea water intrusion in coastal aquifers. Ground Water. 2009; 47(2): 197-204.

[2] Haddout S, Maslouhi A. Two-dimensional modeling of the vertical circulation of salt intrusion in the Sebou estuary under different hydrological conditions. ISH Journal of Hydraulic Engineering. 2017.
[3] Xiao Y, Liu J, Yang SF, Li WJ. Impact of channel deepening on the saltwater intrusion process in the Qinjiang River estuary, Southeast China. Estuarine, Coastal and Shelf Science. 2024; 300: 108718.
[4] Ouda AS. Effect of Superplasticizer Dosage on Compressive Strength and Microstructure of High Volume Basic-Oxygen Slag Mortar Exposed to Sea Water Attacks. Journal of Civil Engineering and Construction. 2021;10(1):11-20.
[5] Xiong Z, Farazdaghi E, Jeong J, Guillou N, Chapalain G. Sea Surface Salinity Forecasting with a Comparison Studying Case of GMM-VSG and FB-Prophet Model. Journal of Civil Engineering and Construction.2024;13(1): 12-28.
[6] Wullems BJM, Brauer CC, Baart F, et al. Forecasting estuarine salt intrusion in the Rhine-Meuse delta using an LSTM model. Hydrology and Earth System Sciences.2023;27: 3823-3850.
[7] Ysebaert T, Van Der Hoek DJ, Wortelboer R, Wijsman JWM, Tangelder M, et al. Management options for restoring estuarine dynamics and implications for ecosystems: A quantitative approach for the Southwest Delta in the Netherlands. Ocean & Coastal Management. 2016; 121: 33-48.
[8] Pauw P, De Louw PGB, Oude Essink GHP. Groundwater salinisation in the Wadden Sea area of the Netherlands: quantifying the effects of climate change, sea-level rise and anthropogenic interferences. Netherlands Journal of Geosciences - Geologie en Mijnbouw. 2012; 91(3): 373-383.
[9] Bhattachan A, Emanuel RE, Ardón M, Bernhardt ES, Anderson SM, et al. Evaluating the effects of land-use change and future climate change on vulnerability of coastal landscapes to saltwater intrusion. Elem Sci Anth.2018; 6: 62.
[10] Feldman RL. Recommendations for responding to sea level rise: Lessons from North Carolina. Solutions to Coastal Disasters. 2008;15-27.
[11] O'Donnell KL, Bernhardt ES, Yang X, Emanuel RE. Saltwater intrusion and sea level rise threatens U.S. rural coastal landscapes and communities. Anthropocene. 2024; 45: 100427.
[12] Gong W, Shen J. The response of salt intrusion to changes in river discharge and tidal mixing during the dry season in the Modaomen Estuary, China. Continental Shelf Research. 2011;31(7): 769-788.
[13] Liu B, Peng S, Liao Y, Wang H. The characteristics and causes of increasingly severe saltwater intrusion in Pearl River Estuary. Estuarine, Coastal and Shelf Science, 2019, 223: 86-98.
[14] Kuang C, Jiang M, Huang J, Gu J. Numerical simulation of impact of the upstream discharge on salinity at Qingcaosha Reservoir.In:Proceedings of the 2011 IEEE International Conference on Mechatronics and Automation. IEEE. 2011: 2334-2337.
[15] Zhang W, Wang Y, Yang T, Huang H. The temporal and spatial evolution of saltwater intrusion during dry season in the Yangtze River Estuary, China. Advanced Materials Research.2014;1010-1012: 1099-1103.
[16] Liu B, Yan S, Chen X, Lian Y, Xin Y. Wavelet analysis of the dynamic characteristics of saltwater intrusion — A case study in the Pearl River Estuary of China. Ocean & Coastal Management. 2014; 95: 81–92.
[17] Xu KQ, Wu P, Yang SF, Hu J, Liao JH. Numerical Investigation of Salt Water Intrusion in Qingnian Reservoir of Pinglu Canal.Port & Waterway Engineering. 2025;(6): 7-12.
[18] Chongqing Jiaotong University. Pinglu Canal engineering feasibility study report- study on the impact of seawater intrusion at Qingnian Reservoir .Chongqing,China.2022.
[19] Chongqing Jiaotong University.General report on the study of engineering measures and effectiveness for mitigation of saltwater intrusion at the Pinglu Canal Qingnian navigation complex. Chongqing,China.2023.
[20] Chaiyarit J, Tuvayanond W, Intarasaksit P. Factors associated with the quality of life of people living in saltwater intrusion areas. Unnes Journal of Public Health. 2025; 14(2): 115-124.
[21] Keulegan GH. Twelfth progress report on model laws for density currents: The motion of saline fronts in still water. Washington: U.S. Dept. of Commerce, National Bureau of Standards. 1958.
[22] Benjamin TB. Gravity currents and related phenomena. Journal of Fluid Mechanics. 1968; 31(2): 209-248.
[23] Simpson JE. Gravity Currents in the Laboratory, Atmosphere, and Ocean. Annual Review of Fluid Mechanics. 1982; 14(1): 213-234.
[24] Turner JS. Buoyancy Effects in Fluids. Cambridge University Press. 1973.
[25] Li YZ. Saltwater wedge gravity current intrusion of sea locks and the air curtain saltwater prevention system for Xingang Lock. Port & Waterway Engineering. 1982;(05): 23-28.
[26] Zhou HX. Seawater intrusion of estuarine locks and its prevention. Advances in Science and Technology of Water Resources. 1994;(02): 48-55.
[27] Yin X, He Y, Lu C, Gao S, Liu Q. Experimental study on front spreading of lock-exchange gravity current with long lock length. Journal of Engineering Mechanics. 2020; 146(1): 04019113.
[28] Lin YD, Liu YY, Yuan YP. Effects of vegetation patches on gravity currents in stratified and non-stratified environments. Journal of Jilin University (Earth Science Edition). 2019; 49(06): 1714-1722.

[29] Xie XY, Han DR, Lin YD. Numerical simulation of effects of rigid vegetation patches on gravity currents in stratified environments. Hydro-Science and Engineering. 2022;(01): 77-88.
[30] Han DR, Yu JY, Yuan YP, et al. Effects of rough bed on mixing and turbulence characteristics of continuous inflow gravity currents. Journal of Shanghai Jiao Tong University. 2021; 55(01): 77-87.
[31] Xu KQ, Liao JH, Yang SF, Wu P, Zhang P, et al. Impact of hip motion-induced single disturbance on gravity currents using particle image velocimetry and planar laser-induced fluorescence techniques. Physics of Fluids.2025; 37(1):015184.
[32] Xu KQ, Liao JH, Yang SF, Wu P, Zhang P, et al. An experimental investigation into density field mixing caused by ship motion in a two-layer density-stratified environment. Ocean Engineering. 2025; 333:121504.
[33] Jiang ZB, Lu H, Yang QY. Three-dimensional numerical simulation of seawater intrusion into freshwater canals via navigation locks. Journal of Yangtze River Scientific Research Institute. 2016; 33(02): 52-56.
[34] Liang XL, Qiao WL, Zhao XZ. Direct numerical simulation of gravity currents in stratified environments. Journal of Zhejiang University (Engineering Science). 2018; 52(05): 996-1001+1013.
[35] Cantero MI, Lee JR, Balachandar S, Garcia MH. On the front velocity of gravity currents. Journal of Fluid Mechanics. 2007; 586: 1-39.
[36] Cantero MI, Balachandar S, Garcia MH. High-resolution simulations of cylindrical density currents. Journal of Fluid Mechanics. 2007; 590: 437-469.
[37] Xu KQ, Liao JH, Yang SF, Wu P, Hu J. Numerical investigation of saline gravity currents with different water depth and salinity based on the lattice Boltzmann method. Physica Scripta. 2024; 99(10):105281.
[38] Huang C. Impact of the Yangtze estuary deepwater channel project on saltwater intrusion. Water Resources and Power. 2019; 37(03): 29-32.
[39] Ding L, Chen LM, Gao XY, Chen YH, Wang YF, et al. Response of salinity at water intake in the Yangtze estuary to runoff-tide dynamics. Hydro-Science and Engineering. 2018;(05): 14-23.
[40] Dai A, Huang YL. The flow within the head of a gravity current. Journal of Fluid Mechanics. 2024; 997: A42.
[41] Dai A, Huang YL, Wu CS. Energy balances for the collision of gravity currents of equal strengths. Journal of Fluid Mechanics. 2023; 959: A20.
[42] Zhu R, He Z, Meiburg E. Mixing, entrainment and energetics of gravity currents released from two-layer stratified locks. Journal of Fluid Mechanics. 2023; 960: A1.
[43] Zhang P. Experimental study on the mechanism of saltwater intrusion in estuary with runoff and tide. Guangzhou: South China University of Technology.2017.